

# Rapid fabrication of mini droplet lens array with tunable focal length

Bo Dai (戴博), Huansi Wang (王奂思), Qiao Xu (徐巧), Zhenqing Li (李振庆),  
Chunxian Tao (陶春先), and Dawei Zhang (张大伟)\*

*Engineering Research Center of Optical Instrument and System, Ministry of Education and Shanghai Key Laboratory of Modern Optical System, University of Shanghai for Science and Technology, Shanghai 200093, China*

\*Corresponding author: dwzhang@usst.edu.cn

Received May 29, 2018; accepted November 1, 2018; posted online November 28, 2018

A rapid and cost-effective method for fabricating mini lens arrays is proposed. The lenses are made of silicone oil droplets and filled inside a polydimethylsiloxane (PDMS) elastomer. The lens arrays of different initial focal lengths and apertures can be fabricated by using the droplets of different volumes. Due to good elastic behavior of PDMS, the droplet lenses can be flexibly deformed, and the focal length and numerical aperture can be tuned by applying an external force on the PDMS elastomer. Furthermore, an apparatus for focal length tuning is designed and employed in the imaging system.

OCIS codes: 220.0220, 220.3630.

doi: 10.3788/COL201816.122201.

In the traditional manufacture of glass or silica optical lenses, milling techniques are widely used. The techniques can precisely fabricate the lenses of complex structures. Nevertheless, the whole fabrication process including cutting, grinding, and polishing is time consuming. It requires professional engineers to design the lenses and skillful technicians to operate high-cost facilities for lens fabrication. In addition, the lenses produced by the milling method have a fixed focal length.

Various techniques have been proposed to fabricate focal-length-tunable lenses. The focal length tuning can be realized by either adjusting the refractive index of the lens<sup>[1,2]</sup> or changing the shape of the lens<sup>[3-5]</sup>. In the liquid crystal lens, a lens is bonded with a liquid crystal layer. The focal length can be well controlled by applying an electrical field on the liquid crystal layer to reorganize the distribution of the refractive index<sup>[6,7]</sup>.

Liquid lenses can be fabricated by infusing high-refractive-index liquid into a chamber. An elastic membrane tightly seals the lens chamber<sup>[8,9]</sup>. By squeezing the chamber, the curvature of the elastic membrane can be adjusted, and the tuning of the focal length can be realized. In Ref. [10], the chamber was designed as a communicating vessel and sealed by an elastic membrane and a photo-polymer. The deformation of the photo-polymer driven by UV light could indirectly bend the elastic membrane and tune the focal length. The mechano-fluidic technique provides an alternative way for focal length tuning<sup>[11,12]</sup>. By controlling the volume of the liquid in the chamber, the elastic membrane could be deformed, and the focal length could be tuned. Besides sealing liquid in a chamber covered by an elastic membrane, a liquid lens can be formed by using two immiscible liquids. Focal length tuning can be realized by the electrowetting technique for manipulating the interface of the liquids<sup>[13,14]</sup>. Nevertheless, the interface of the liquids might be

deformed by the external undesired force, such as the gravity effect, when the lens is placed at a vertical position, and the lens made of the liquid phase would be affected. As a result, the imaging quality degrades due to the deformation of the lens profile.

Recently, a novel liquid-filled droplet lens was proposed<sup>[15]</sup>. In the fabrication of the lens, a high-refractive-index and high-density droplet sinks to the bottom of a liquid-state polymer of relatively low refractive index and low density. Once the forces applied to the droplet, i.e., tension force, gravity, buoyant force, and normal force, are balanced, the polymer is solidified to an elastomer, and the plano-convex-shaped droplet at the bottom of the elastomer is still in a liquid state, forming a mini lens. The focal length can be flexibly and widely tuned by squeezing the elastomer.

Lens arrays are essential optical components widely used in lots of applications, such as three-dimensional (3D) imaging, 3D display<sup>[16]</sup>, multispectral imaging<sup>[17]</sup>, and efficiency enhancement for photovoltaic cells<sup>[18,19]</sup>. Lens arrays can be fabricated by many techniques, including thermal reflow<sup>[20]</sup>, laser direct writing<sup>[21,22]</sup>, inkjet printing<sup>[23]</sup>, and photolithography<sup>[24]</sup>. The thermal reflow technique can rapidly produce a lens array by melting an array of pre-prepared cylindrical polymers into a hemispherical shape. To have a complex profile of lenses, the laser direct writing technique can be used to realize 3D structural modification. Besides, the inkjet printing technique can print out lenses one by one according to a pre-defined program, and the curvature of the lenses can be controlled by the surface modification of the substrate. The photolithography technique can directly fabricate an array of highly uniform lenses by transferring a pattern of a lens-array structure from a gray-scale mask to photo-resist. Although the techniques can fabricate high-quality lens arrays, the focal length of the lenses can only be

determined during the fabrication stage and cannot be tuned once the lens arrays are developed.

In this Letter, a rapid fabrication technique to produce mini droplet lens arrays is proposed. The focal length of the lenses can be flexibly adjusted by squeezing the lens array. Optical imaging is demonstrated by using the fabricated focal-length-tunable mini lens array.

Figure 1(a) illustrates the fabrication process of the droplet lens array. A PMMA mold with an array of holes is firstly prepared by laser cutting. The mold has the thickness of about 1 mm. Then, the mold is placed on a glass plate (N-BK7, refractive index: 1.515), which is at the bottom of a container. Liquid-state polydimethylsiloxane (PDMS) (density:  $0.965 \text{ g/cm}^3$ ) is poured into the container to submerge the mold by 1 mm. To realize a low Young's modulus and a good elastic behavior of the PDMS, the PDMS solution is prepared with a 15:1 mass ratio of the silicone elastomer and the curing agent<sup>[25]</sup>. After that, a high-accuracy syringe pump (Harvard Apparatus PHD 2000) is used to push a syringe connected with a silica capillary to generate silicone oil droplets. Silicone oil has refractive index of 1.579 and density of  $1.100 \text{ g/cm}^3$ . The silica capillary is mounted on a two-dimensional moving stage. By controlling the position of the silica capillary, the droplets can be precisely dripped into the different holes of the mold. When the droplet sinks to the bottom and the force equilibrium is achieved, the upper surface of the droplet has a convex shape, and the lower surface is flat. A mini plano-convex droplet lens is formed. After all the holes are filled with the silicone oil droplets, the container is placed into an oven to heat the PDMS at  $80^\circ\text{C}$  for 2 h. Finally, the solidified PDMS containing a droplet lens array is taken out of the container. The solidified PDMS has refractive index of 1.403.

A fabricated  $4 \times 4$  mini lens array is shown in Fig. 1(b). The size of the lens array is  $5.5 \text{ mm} \times 5.5 \text{ mm} \times 2 \text{ mm}$  (length  $\times$  width  $\times$  thickness). Each lens is made of a

$1.6 \mu\text{L}$  silicone oil droplet in the hole of 1 mm diameter. The separation of the lenses is  $100 \mu\text{m}$ . The size of the lens array can be significantly reduced if small droplets can be generated and a mold of small size is used. The inkjet printing technique can produce droplets in the scale of micrometers<sup>[26]</sup>, and a small mold can be fabricated by using a high-precision laser cutting technique or photolithography technique. The lenses are uniform and have smooth convex surfaces. The focal length and the numerical aperture (NA) of the lenses are 2.18 mm and 0.25, respectively.

Figure 2 shows the entire process of the sinking of a silicone oil droplet. The droplet firstly overcomes the surface tension of the PDMS surface and moves downwards. It takes about 2 min for the droplet to completely penetrate the surface. Since the gravity of the droplet is large enough to overcome the buoyant force and viscous resistance of the PDMS, the droplet keeps sinking. The large viscous resistance makes the droplet sink slowly. After the droplet sinks to the bottom of the hole, it takes 3 min for stabilization by balancing gravity, buoyant force, normal force, and tension force. Finally, the droplet with a curved surface occupies the bottom of the hole.

In addition, to investigate the tolerance of the fabrication, the silica capillary aims a 1 mm diameter hole with a deviation from the center by  $200 \mu\text{m}$ . The droplet sinks towards the hole away from the center, as shown in Fig. 3. When hitting the rim of the hole, the droplet deforms but does not break up. After that, the droplet slips into the hole as a whole, and a mini lens can be formed. It indicates that the mold used in the fabrication can efficiently avoid misalignment. Besides that, if the mold is not used, the droplets at the bottom of the PDMS would be pushed away by the sinking droplets. Thus, the mold is indispensable in the fabrication of the droplet-filled lens array.

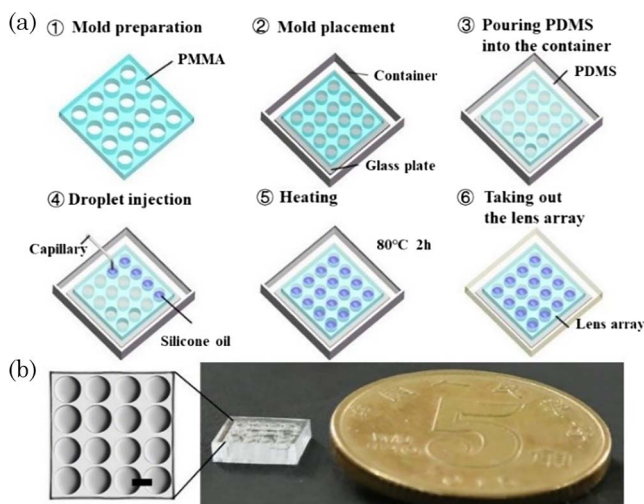


Fig. 1. (a) Fabrication process of the droplet-filled convex lens array. (b) Photo of the fabricated lens array and the top-view microscopic image of the lens array.

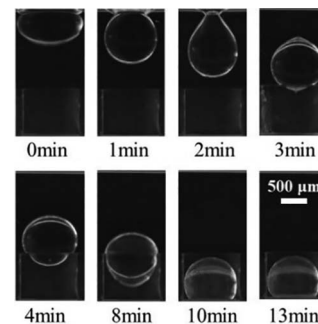


Fig. 2. Sinking process of the silicone oil droplet.

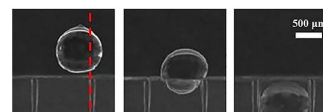


Fig. 3. Sinking of the silicone oil droplet with a deviation from the center.

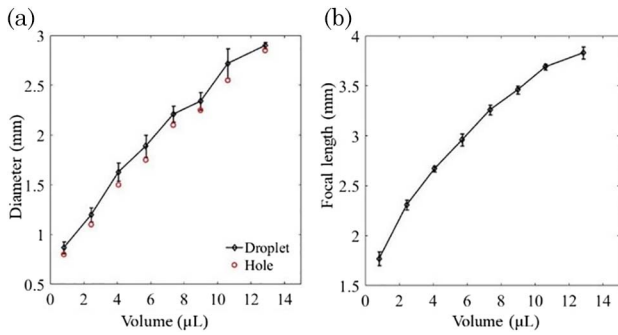


Fig. 4. (a) Relation of the droplet volume and the diameter of the droplet at the bottom of the PDMS without the mold. The designed holes are slightly smaller than the diameter of the droplet. (b) Focal length of the lenses made of silicone oil droplets with different volumes.

Figure 4(a) shows the relation between the volume of the droplet and the size of the droplet at the bottom of the PDMS without using the mold. The error bar indicates the standard deviation of ten different experimental trials. The droplet of different volumes is produced by using the silica capillary of different sizes. With the increase of the droplet volume, the diameter of the droplet becomes large. The deviation of the droplet diameter is about 6.7%. To ensure uniform alignment and identical size of the lenses, the diameter of the holes is designed slightly smaller than that of the droplet in the PDMS. The size of the hole, corresponding to the aperture of the lens, varies from 0.8 to 2.8 mm.

The focal length of the lenses is experimentally measured, as shown in Fig. 4(b). In the experiment, a 633 nm collimated laser beam passes through the lens array, and a beam profiler mounted on a precision translation stage behind the lens array is used to search the focal points along the propagation direction. The focal length increases from 1.77 to 3.83 mm with the change of the droplet volume from 0.82 to 12.84  $\mu\text{L}$ . The deviation of the focal length of the lenses on the same lens array is less than 6%, which is mainly resulted from the non-uniform holes of the PMMA mold. In addition, the error bar in Fig. 4(b) stands for the standard deviation of the focal length of the ten lens arrays. The difference of the lens arrays is 6.9%, which is determined by comparing the ten lens arrays with the average focal length of the lenses. The uniformity of the lenses can be improved by employing high-precision laser cutting for producing holes with vertical walls.

The droplet lenses inside the solidified PDMS elastomer can be easily deformed by applying a force on the PDMS. Thus, the curvature of the interface of the silicone oil and PDMS can be manipulated. Figure 5(a) shows focal length tuning of the two lens arrays by applying a force vertically on the PDMS. The PDMS has Young's modulus of about 400 to 600 kPa and exhibits a good elastic behavior. The height of the droplet lenses is reduced, and the curvature of the lenses becomes small. The elastic deformation of the PDMS is about 1 mm. The focal length monotonically

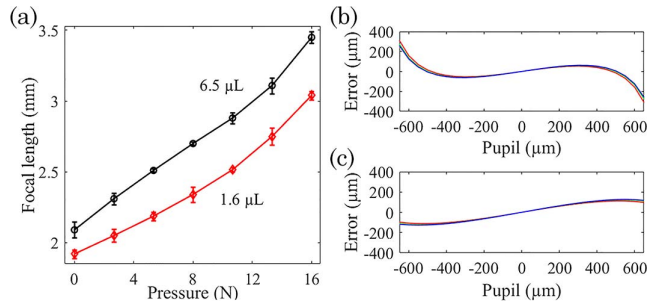


Fig. 5. (a) Focal length tuning of the lens array. Ray fan diagrams for analyzing the aberration of the lens made of a 6.5  $\mu\text{L}$  droplet (b) without pressure and (c) with 16 N pressure. Blue, 486 nm; green, 588 nm; red, 656 nm.

changes from 1.92 to 3.04 mm and from 2.17 to 3.45 mm for the lens arrays made of 1.6 and 6.5  $\mu\text{L}$  droplets. The error bar indicates the stability of the focal length tuning. If the applied force is the same, the deviation of the focal length is within 1.6%. The corresponding NA varies from 0.25 to 0.16 and from 0.46 to 0.29, respectively.

The aberration for the lens made of a 6.5  $\mu\text{L}$  droplet is calculated by using ZEMAX software based on the profile of the lens, as shown in Figs. 5(b) and 5(c). The input light is at 486, 588, and 656 nm, respectively. Spherical aberrations can be observed in the ray fan diagrams. In comparison, when the lens is squeezed by the pressure of 16 N, the aberration is reduced. Besides, the curves representing the light of different wavelengths almost overlap each other, indicating small chromatic aberration.

An optical imaging experiment is conducted to evaluate the optical performance of the lens array. The setup of the imaging system is shown in Fig. 6(a). A white-light light emitting diode (LED) is used to illuminate a mask, where there is a letter 'A'. The lens array is sandwiched by two glass plates and placed in a customized lens mount, as shown in Fig. 6(b). By rotating the cap of the lens mount, the lens array is vertically squeezed, and the focal length can be adjusted. The lens array can be squeezed with the

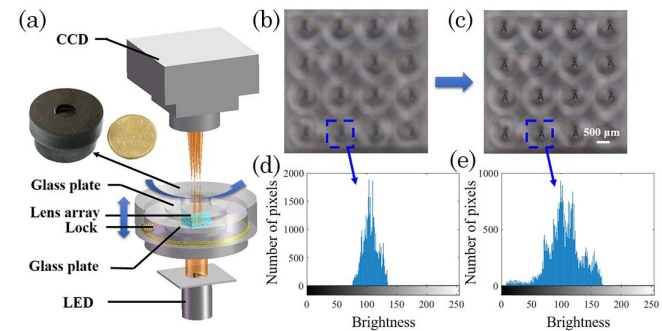


Fig. 6. (a) Imaging system for evaluating the imaging performance of the lens array. Inset: the customized lens mount. The image array of the letters (b) before and (c) after the tuning. The contrast of the image formed by a lens (d) before and (e) after the tuning.

resolution of  $1.39\ \mu\text{m}/\text{degree}$ , and the total deformation is about  $800\ \mu\text{m}$ . The lens array used in the experiment is made of  $1.6\ \mu\text{L}$  droplets. A CCD camera behind the lens array has a fixed focal length and attempts to capture the image on the focal plane of the lens array. The focal length of the lens array is tuned to ensure that the focal planes of the camera lens and the lens array are on the same level. When the lens array is not squeezed, the lenses have large spherical aberrations, the focal plane of the lenses is out of the focus of the camera lens, the image is blurred, and the letter is hard to recognize, as shown in Fig. 6(b). With the adjustment of the focal length, the image is in focus, and the aberration is reduced. The blurry image becomes clear, and the letter cluster can be recognized, as illustrated in Fig. 6(c). Figs. 6(d) and 6(e) indicate that the contrast of the image is improved after the tuning of the lens array. The letters observed by the lenses on the perimeter of the lens array are not at the center of the lenses because the letter on the mask is away from the optical axes of the lenses. The mold used in the lens array leads to penumbra in the image, but it has very low influence over the imaging. The letters are clearly readable, indicating good optical performance of the fabricated lens array.

In conclusion, a rapid fabrication technique for producing focal-length-tunable lens array is proposed. High-refractive-index and high-density silicone oil droplets sink to the bottom of liquid-state PDMS and form convex lenses with a curved interface between the silicone oil and the PDMS. The focal length and aperture of the lenses can be controlled by using different-sized silica capillaries to generate the droplets of different volumes. The deviation of the fabrication is less than 6.9%. Furthermore, the solidified PDMS has the property of elastic deformation. By applying an external force vertically on the lens array, the focal length of the lens array could be flexibly extended by about 50%. In the demonstration of optical imaging, the fabricated lens array placed in a customized lens mount is used for focal length tuning, and a clear image array is obtained at the focal plane. The proposed fabrication technique could be an efficient way to produce diverse tunable optical components.

The work was supported by the National Key Research and Development Program of China (No. 2016YFD0500603), the National Natural Science

Foundation of China (Nos. 61601292 and 61775140), and the Shanghai Science and Technology Commission (Nos. 17060502500 and 17JC1400601).

## References

1. S. U. Kim, S. Lee, J. H. Na, and S. D. Leen, *Opt. Commun.* **313**, 329 (2014).
2. S. J. Hwang, Y. X. Liu, and G. A. Porter, *Opt. Express* **21**, 30731 (2013).
3. G. H. Feng and J. H. Liu, *Appl. Opt.* **52**, 829 (2013).
4. S. Kuiper and B. H. W. Hendriks, *Appl. Phys. A* **85**, 1128 (2004).
5. L. Wang, T. Hayakawa, and M. Ishikawa, *Opt. Express* **25**, 31708 (2017).
6. H. Ren, D. Ren, and S. Wu, *Opt. Express* **17**, 24183 (2009).
7. H. Ren and S. Wu, *Opt. Express* **14**, 11292 (2006).
8. L. Wang, H. Oku, and M. Ishikawa, *Opt. Express* **22**, 19448 (2014).
9. L. Wang, H. Oku, and M. Ishikawa, *JPN J. Appl. Phys.* **56**, 122501 (2017).
10. S. Xu, H. Ren, Y. J. Lin, M. G. J. Moharam, S. T. Wu, and N. Tabiryan, *Opt. Express* **17**, 17590 (2009).
11. A. Tripathi, T. V. Chokshi, and N. Chronis, *Opt. Express* **17**, 19908 (2009).
12. N. Chronis, G. Liu, K. H. Jeong, and L. P. Lee, *Opt. Express* **11**, 2370 (2003).
13. H. Choi and Y. Won, *Opt. Lett.* **38**, 2197 (2013).
14. L. Li, C. Liu, H. Ren, H. Deng, and Q. Wang, *Opt. Lett.* **40**, 1968 (2015).
15. C. Fang, B. Dai, R. Zhuo, X. Yuan, X. Gao, J. Wen, B. Sheng, and D. Zhang, *Opt. Lett.* **41**, 404 (2016).
16. Y. Wang, Q. H. Wang, D. H. Li, H. Deng, and C. G. Luo, *Chin. Opt. Lett.* **11**, 061101 (2013).
17. R. Shogenji, Y. Kitamura, K. Yamada, S. Miyatake, and J. Tanida, *Opt. Express* **12**, 1643 (2004).
18. M. Cho and M. Danshanah, *Proc. IEEE* **99**, 556 (2010).
19. K. Tvingstedt, S. D. Zilio, O. Inganäs, and M. Tormen, *Opt. Express* **16**, 21608 (2008).
20. M. He, X. C. Yuan, N. Q. Ngo, J. Bu, and V. Kudryashov, *Opt. Lett.* **28**, 731 (2003).
21. C. H. Lin, L. Jiang, Y. H. Chai, H. Xiao, S. J. Chen, and H. L. Tsai, *Appl. Phys. A* **97**, 751 (2009).
22. A. Pan, T. Chen, C. X. Li, and X. Hou, *Chin. Opt. Lett.* **14**, 052201 (2016).
23. J. Y. Kim, N. B. Brauer, V. Fakhfour, D. L. Boiko, E. Charbon, G. Grutzner, and J. Brugger, *Opt. Mater. Express* **1**, 259 (2011).
24. Q. Peng, Y. Guo, S. Liu, and Z. Cui, *Opt. Lett.* **27**, 1720 (2002).
25. D. Fuard, T. T. Chevolleau, S. Decossas, P. Tracqui, and P. Schiavone, *Microelectron. Eng.* **85**, 1289 (2008).
26. Y. Luo, L. Wang, Y. Ding, H. Wei, X. Hao, D. Wang, Y. Dai, and J. Shi, *Appl. Surf. Sci.* **279**, 36 (2013).